

www.acsami.org Research Article

Chemical Sulfide Tethering Improves Low-Temperature Li—S Battery Cycling

David A. Burns, Avery E. Baumann, Kevin J. Bennett, José C. Díaz, and V. Sara Thoi*



Cite This: ACS Appl. Mater. Interfaces 2021, 13, 50862–50868



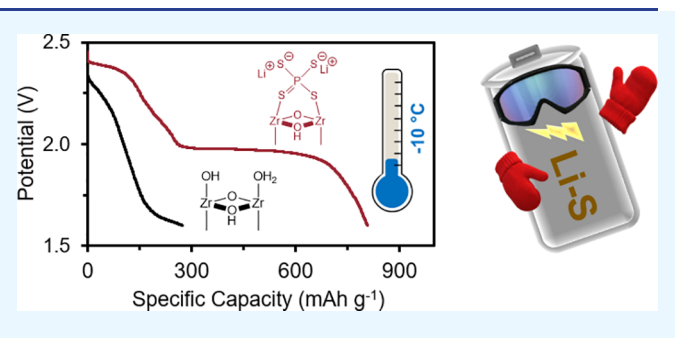
ACCESS

III Metrics & More

Article Recommendations

s Supporting Information

ABSTRACT: Demands for energy storage and delivery continue to rise worldwide, making it imperative that reliable performance is achievable in diverse climates. Lithium—sulfur (Li—S) batteries offer a promising alternative to lithium-ion batteries owing to their substantially higher specific capacity and energy density. However, improvements to Li—S systems are still needed in low-temperature environments where polysulfide clustering and solubility limitations prohibit complete charge/discharge cycles. We address these issues by introducing thiophosphate-functionalized metal—organic frameworks (MOFs), capable of tethering polysulfides, into the cathode architecture. Compared to cells with the parent



MOFs, cells containing the functionalized MOFs exhibit greater capacity delivery and decreased polarization for a range of temperatures down to -10 °C. We conduct thorough electrochemical analyses to ascertain the origins of performance differences and report an altered Li–S redox mechanism enabled by the thiophosphate moiety. This investigation is the first low-temperature Li–S study using MOF additives and represents a promising direction in enabling energy storage in extreme environments.

KEYWORDS: batteries, electrochemical cells, lithium, sulfur, metal-organic frameworks

o accommodate an increasingly electrified society, it is paramount that energy storage devices are able to operate safely and reliably in a variety of climates. Widespread adoption of battery-powered electric vehicles is particularly challenged by poor driving range at low temperatures (near or below 0 °C), where charge storage and power output of current Li-ion batteries are severely diminished. 1,2 Complex thermal systems are generally used to warm the battery in these environments, which consume energy that could otherwise be used for vehicle operation.^{3,4} Removing the need for external heaters would enable more efficient use of space and energy in the system. Furthermore, expanding applications into batterypowered space-, air-, and seacraft for commercial and military use will necessitate operation in extreme environments with temperatures far below 0 °C. Advanced batteries beyond Li-ion technologies may offer a solution to the rising needs for lowtemperature energy storage.

Lithium–sulfur (Li–S) batteries are desirable as an alternative to incumbent Li-ion technologies owing to a high theoretical energy density (\sim 2600 Wh kg⁻¹) that enables longer device operation between charges. The high energy density is attained by converting neutral sulfur (S₈) to fully reduced Li₂S, which is a 16-electron process involving discrete polysulfide equilibria. Si,6 At low temperatures, however, Li–S batteries struggle to fully charge and discharge due to strong cell polarization (resistance within the cell) arising from poor charge transfer and slow ionic mobility (Scheme 1, left). The reduction of Li₂S₄ to Li₂S is particularly difficult at cold

temperatures due to the low solubility of $\mathrm{Li}_2\mathrm{S}_x$ in conventional electrolytes, restricting the discharge process and limiting the electrical output upon precipitation. Furthermore, the accumulation of $\mathrm{Li}_2\mathrm{S}_4$ encourages the formation of strongly aggregated clusters, which hinders the electrochemical accessibility of the active sulfur species. These issues worsen as the temperature decreases, thus presenting significant challenges to implementing high-capacity Li -S batteries in frigid climates.

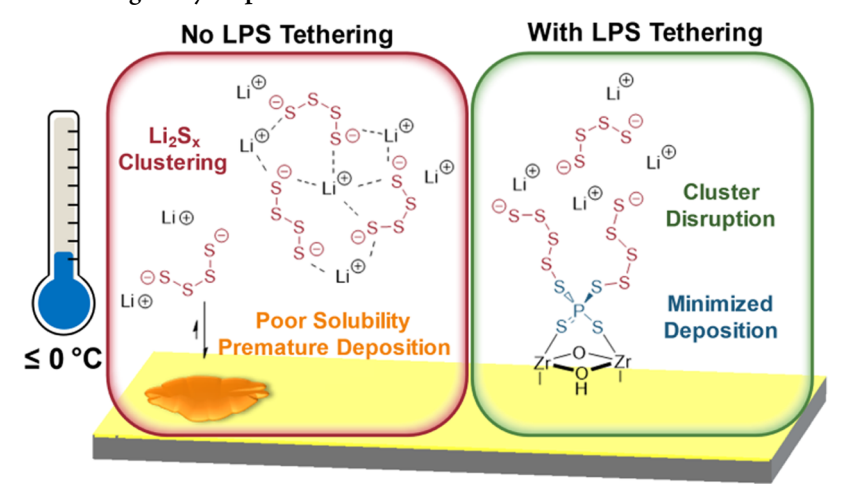
To date, there have been very few studies on the Li–S battery charge/discharge at low temperatures. The one strategy to improve cycling performance is to optimize the electrolyte composition. Other efforts have focused on functionalized cathode materials to trap or attract Li_2S_x near the electrode surface to maximize sulfur utilization. The such study promoted the conversion of Li_2S_x at 0 °C by installing MnS nanoparticles as chemisorption sites in the sulfur cathode. Another study utilized a two-dimensional (2D) MoSe layered material with edge sites that aid in adsorption and catalytic reduction and oxidation of Li_2S_x at 0

Received: June 28, 2021 Accepted: October 6, 2021 Published: October 20, 2021





Scheme 1. Reduced Temperatures Limit Electrochemical Access to Li,S., Species via Polysulfide Clustering and Poor Solubility, Chemical Tethering via Lithium Thiophosphate (LPS) Improves Electrochemical Accessibility by Disrupting the Polysulfide Clusters and Preventing Early Deposition



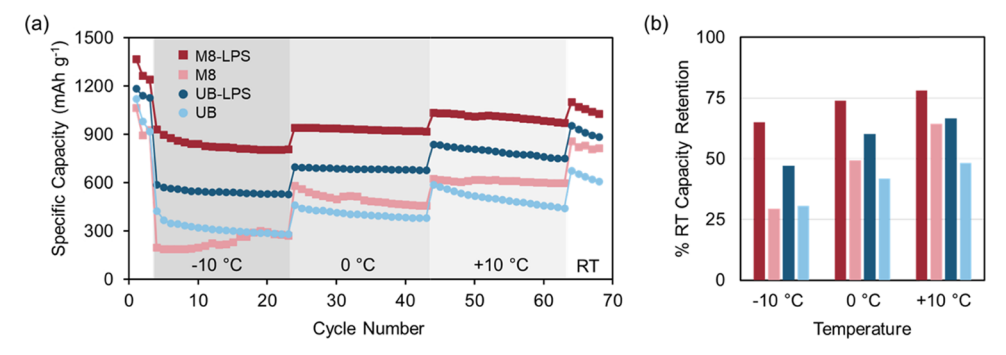


Figure 1. (a) Discharge capacity for each cycle at various temperatures. All cells were cycled at a rate of C/10 (168 mA g⁻¹) 3 times at 22 °C ("RT", to prime the cell), 20 times at all reduced temperatures (-10 °C, 0 °C, 10 °C), and then 5 times at RT. (b) Comparative performance of the capacity of each cell across the examined temperature range relative to the initial capacity at RT. The LPS-functionalized MOFs facilitate cycling, enabling higher absolute and relative capacities than their unfunctionalized counterparts.

and −25 °C. 16 The best performance reported to date was achieved using graphene-supported boron nitride (BN) nanosheets to promote the strong adsorption of Li₂S_x at the BN edge sites, enabling operation at temperatures from -40 to 70 °C. 11 It also has been suggested that limiting undesirable Li_2S_x film deposition, which is prevalent at low temperatures, mitigates passivation of the cathode surface. 19,20 Motivated by these studies, we leveraged the advantages of chemical tethering to improve the capacity delivery for Li-S batteries operating at low temperatures.

We, among others, have demonstrated the efficacy of covalently tethering Li₂S_x to metal-organic frameworks (MOFs) and covalent organic frameworks (COFs) in composite cathodes to improve battery performance at ambient temperature.²¹⁻²⁴ Specifically, the incorporation of lithium thiophosphate (LPS) in a Zr-based MOF provided sulfur-anchoring sites and led to decreased cell polarization, higher charge capacity, and superior rate capabilities. 21,23 Based on this previous work, we hypothesized that the ionic LPS tethering group would have similar impacts at reduced temperatures by disrupting polysulfide clusters and preventing Li₂S film deposition (Scheme 1). Herein, we use two different LPS-functionalized MOFs to investigate the influence of chemical tethering on low-temperature Li-S electrochemistry. The MOFs are integrated into composite sulfur cathodes and

explored at a range of temperatures to gain insights into determinants of performance in cold environments.

Two zirconium-based MOFs, UiO-66(50Benz) ("UB", a defected UiO-66 structure) and MOF-808 ("M8"), were selected as candidate materials for this study. Our previous investigation demonstrated that the hexanuclear Zr nodes can be functionalized with LPS, yielding UB-LPS and M8-LPS, respectively.²¹ Owing to the higher number of open sites on the Zr cluster, M8 can incorporate nearly twice the concentration of LPS as UB. To deconvolute contributions arising from purely structural differences in these two data sets, the unfunctionalized "parent" MOFs were also explored in cathodes to benchmark the LPS-functionalized counterparts. The following sections describe the resulting performance differences gleaned from various electrochemical analyses.

Composite cathodes containing sulfur and the MOF additives were prepared and integrated into coin cells with Li metal anodes as described in our previous report.²¹ We selected an electrolyte composition of 0.5 M lithium triflate (LiOTf) and 0.5 M LiNO₃ based on its use in previous studies where temperatures as low as -40 °C were investigated. 7,8,11 The assembled cells were allowed to equilibrate for several hours before undergoing three cycles at room temperature to overcome the difficult first reduction of neutral S₈ to Li_2S_x . 1,1,12,25 After this initiation, the cells were cycled 20 times at each temperature of $-10\,^{\circ}$ C, $0\,^{\circ}$ C, $10\,^{\circ}$ C, and briefly

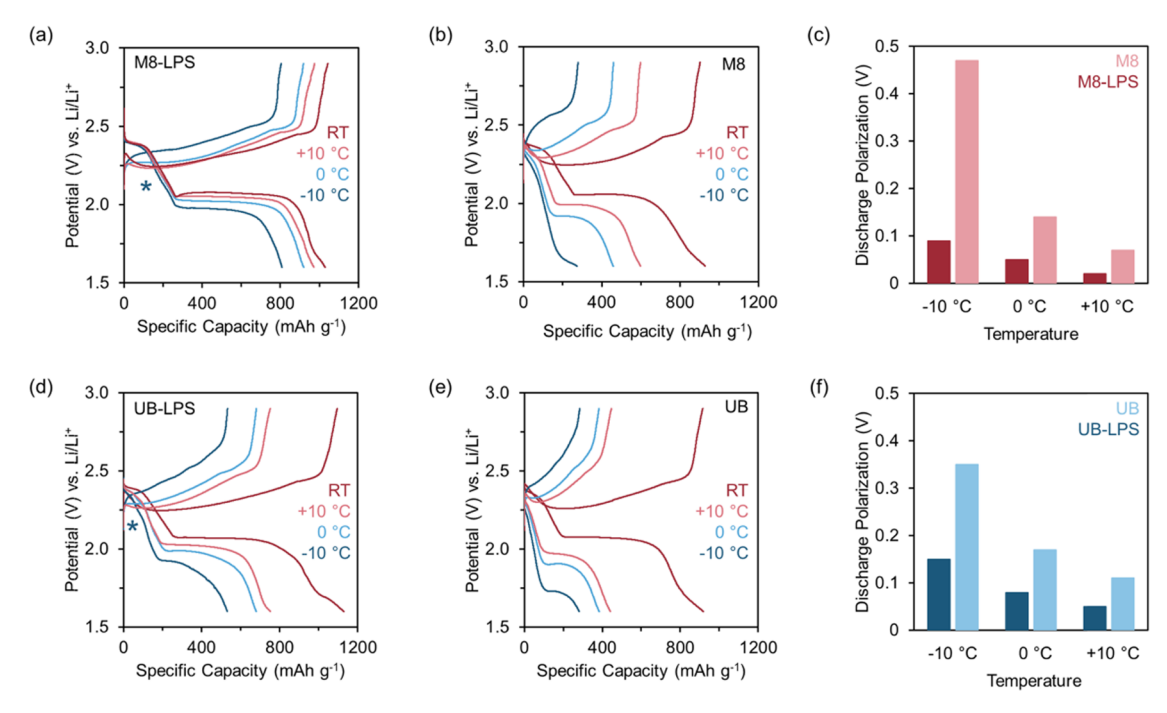


Figure 2. Galvanostatic cycling curves from the final cycle for each temperature at C/10 (168 mA g^{-1}) for (a) M8-LPS, (b) M8, (d) UB-LPS, and (e) UB. Colors correspond to RT (red), +10 °C (light red), 0 °C (light blue), and -10 °C (blue) as indicated in panels (b) and (e). Discharge polarization relative to the RT curve is plotted in (c) and (f). Additional equilibria features discussed in the text are denoted here with an asterisk (*) and displayed more clearly in the Supporting Information (SI).

at 22 $^{\circ}$ C (RT) (Figure 1a). Both charge and discharge processes were conducted at a rate of C/10 (168 mA g⁻¹) at the designated temperature.

The capacities delivered by all cells follow a stepwise behavior as the cycling temperature is increased (Figure 1a), illustrating the electrochemical difficulties inherent to lowtemperature Li-S cycling. Across all temperatures studied, the cells containing the LPS-functionalized MOFs delivered substantially higher capacities than those containing the parent MOFs. After 20 cycles at -10 °C, the lowest temperature studied, cells containing M8-LPS and UB-LPS were able to deliver roughly 810 and 530 mAh g⁻¹, respectively. This improvement is a considerable improvement from the cells without LPS, which both delivered approximately 280 mAh g⁻¹ at -10 °C. Similar differences in capacity were maintained as temperatures increased. In Figure 1b, we plot capacity delivery at lower temperatures relative to room temperature to more clearly visualize the capacity enhancement. It is evident from these results that the LPS moiety improved both absolute and relative capacities across the various conditions studied. The performance of a control cathode containing no MOF is also compared in Figure S1, wherein cells containing M8-LPS and UB-LPS deliver higher relative capacity at all temperatures studied.

Differences in cycling performance prompted us to evaluate the electrochemical profiles of the individual cells. The galvanostatic cycling curves contain a wealth of information about the feasibility of Li-S redox reactions at each temperature, including polarization and polysulfide equilibria (Figure 2). The total cell polarization is made up of a number of factors, including resistance to mass transport, ohmic resistance, and resistance to charge transfer. Stronger degrees of polarization result in lower discharge voltages and higher charge voltages, which limits the power output and cyclability of the cell. The measured cell polarization shows a higher

polarization at lower temperatures for every cell examined (Tables S1 and S2). At -10 °C, the total cell polarization was large enough so that the M8 cell failed to yield a lower plateau above the voltage limit of 1.6 V vs Li/Li⁺ (Figure 2b), while UB eked out a short lower plateau (Figure 2e). In contrast, the galvanostatic profiles from the M8-LPS and UB-LPS cells shown in Figure 2a,d exhibit long, flat plateaus even at -10 °C with only minor variations in potential across the temperature range.

All cells achieved the typical two-plateau behavior at temperatures of 0 $^{\circ}$ C and above, where the decreased polarization permitted the second discharge plateau within the voltage window. The differences in discharge polarization relative to the room temperature profile are compared directly in Figure 2c,f. The clear temperature dependence suggests that the primary difficulties at -10 $^{\circ}$ C are likely related to mass transport and premature deposition of Li₂S_x, both of which are strongly correlated to temperature.²⁷ From the comparative results, it is evident that LPS plays a key role in diminishing cell polarization, particularly for M8-LPS, which has a greater concentration of LPS than UB-LPS.²¹

In addition to polarization effects, we also observe changes to the Li–S cycling mechanism in both the M8-LPS and UB-LPS cells when cycled at $-10\,^{\circ}\mathrm{C}$. A new plateau feature appears during discharge near 2.2 V vs Li/Li⁺ (denoted with * in Figure 2a,d and enlarged in Figure S4), differing from the typical two-plateau behavior. Usually, the upper plateau near 2.4 V vs Li/Li⁺ corresponds to longer-chain Li₂S_x (x > 4), while the lower plateau near 2.1 V vs Li/Li⁺ is made up of the shorter, more reduced Li₂S_x species (x \leq 4). Splitting of the two characteristic plateaus into additional features suggests favorability of extra equilibria, a phenomenon previously reported at $-40\,^{\circ}\mathrm{C}$ with an expanded voltage window, 7 in a cell featuring a polymer electrolyte, 28 and when other species are present to alter the ionic environment of Li⁺. 29 In these

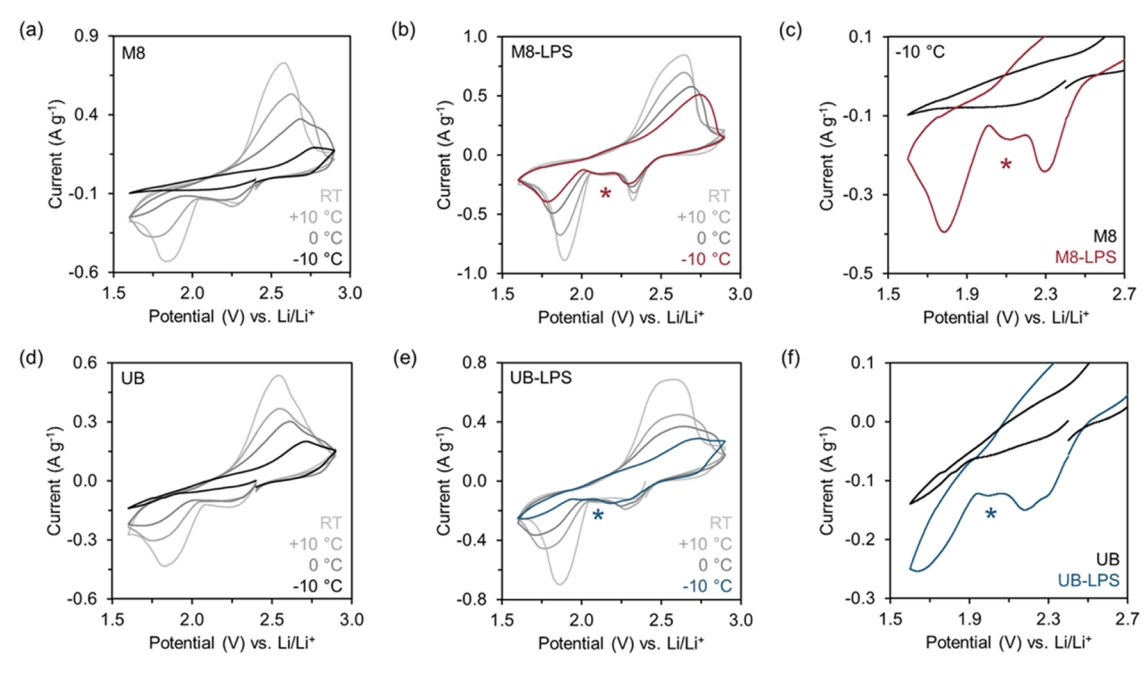


Figure 3. Cyclic voltammetry plots at each temperature for (a) M8, (b) M8-LPS, (d) UB, and (e) UB-LPS. Currents are normalized to the mass of sulfur. The cycle obtained at -10 °C is highlighted in each panel and compared in (c) and (f) showing new features (noted with *) obtained with

cases, the multiplateau behavior was attributed to the stabilization of additional equilibria that would otherwise be

We observed similar multiplateau behavior in our previous study only when LPS-MOF cells were cycled at high C-rates.² We suspect that stabilization of the additional equilibrium is a contributing factor in how UB-LPS and M8-LPS maintain appreciable sulfur utilization in mass transport limited cycling conditions such as fast rates and low temperatures. In the current study, the positioning of the extra discharge feature near 2.2 V vs Li/Li⁺ suggests an additional stabilized reaction step prior to Li₂S₄ formation. The capacity of the two plateau regions at 2.4 and 2.2 V is consistent with the capacity of the concerted single plateau event at RT (Figure 2a,d), further suggesting the partitioning of the electrochemical equilibrium. Thus, we propose the uppermost two discharge plateaus in the LPS cells at -10 °C correspond to the following simplified polysulfide equilibria

$$S_8 \rightleftharpoons Li_2S_8 \rightleftharpoons Li_2S_6 \quad (\sim 2.4 \text{ V})$$

$$\text{Li}_2S_6 \rightleftharpoons \text{Li}_2S_4 \ (\sim 2.2 \text{ V})$$

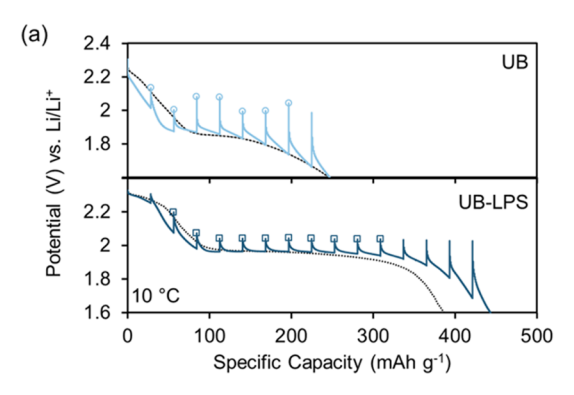
This phenomenon is in contrast with the typical two-plateau behavior, where the upper portion corresponds only with the conversion to Li₂S₄.6 While further experiments are necessary to confirm the chemical species present in the equilibria, we hypothesize the LPS functional group provides favorable covalent and electrostatic stabilization to Li₂S_x at the electrode surface over the bulk electrolyte solution. This interaction consequently influences the equilibration process; the steps of which become more pronounced and observable under unique conditions such as low temperatures. 21,30

To illuminate the altered electrochemical mechanisms, we investigated the behavior with variable temperature cyclic voltammetry (CV) experiments (Figure 3). At 10 °C and RT, all cells exhibit normal behavior with two broad reductive

features near 2.25 and 1.85 V vs Li/Li+, which correspond to the two galvanostatic discharge plateaus. All cells display one wide oxidative feature around 2.6 V vs Li/Li⁺, which corresponds to the broad galvanostatic charge curve. Each of these features shifts to less favorable potentials with decreased temperatures as resistance to charge transfer and mass transport limitations exacerbate cell polarization.

The most distinct differences are observed at -10 and 0 °C, where cells without LPS suffer strong polarization, particularly evidenced by the lack of a second reductive feature within the voltage window. In contrast, the lower potential events, along with additional features highlighted in Figure 3c,f, are observed in both UB-LPS and M8-LPS voltammograms. This observation is in agreement with the multiplateau behavior observed in the galvanostatic cycling experiments described above. Thus, CV further reveals the unique ability of LPS to substantially alter the Li-S redox mechanisms toward pathways that enable sustained cycling performance in extreme

To further probe electrochemical differences among these cells, we apply the galvanostatic intermittent titration technique (GITT), which subjects the cell to pulses of applied current followed by long rest periods. The resulting capacityvoltage profiles obtained at different temperatures (10 °C in Figure 4, RT in Figure S5) provide qualitative information about electrochemical diffusion as well as polarization in the cell.^{31–33} First, we observe polarization effects by comparing the height of the voltage spike from the plateau at each pulse, plotted for clarity in Figure S7. The trends align well with our discussion above regarding polarization, where UB-LPS exhibits smaller and more consistent equilibrium potential differences than UB at all depths of discharge and temperatures. In addition, GITT experiments demonstrate that LPS functionalization led to cells with relatively higher and more constant diffusion coefficients at the second plateau compared to the parent framework. Analysis of the M8 and M8-LPS cells reveals similar relative diffusion coefficient trends (Figure S6)



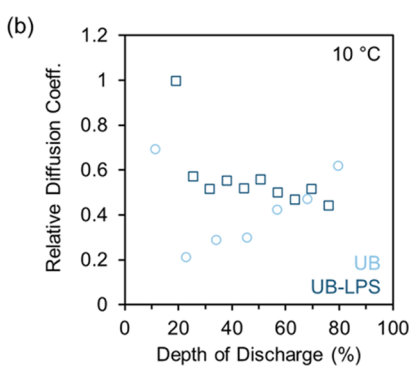


Figure 4. Results from GITT experiments at 10 °C including (a) the discharge profiles comprised of 10 min current pulses and (b) the calculated diffusion coefficients for each marked point, relative to UB-LPS at ~20% depth of discharge.

and polarization values (Figure S7), consistent with our UB/ UB-LPS discussion.

Following our electrochemical analyses, we sought to investigate the ability of thiophosphates to disrupt polysulfide clustering at reduced temperatures. Due to the heterogeneity and low concentration of thiophosphates in the MOF, probing polysulfide clustering directly in the MOF pores was not feasible. Instead, solution ⁷Li NMR spectroscopy of Li₂S₄ solutions in 1:1 (v/v) DOL:DME in the presence and absence of thiophosphates was performed over the range of 15 to -30 $^{\circ}$ C (Figure 5). Owing to the higher solubility of P_2S_5 compared

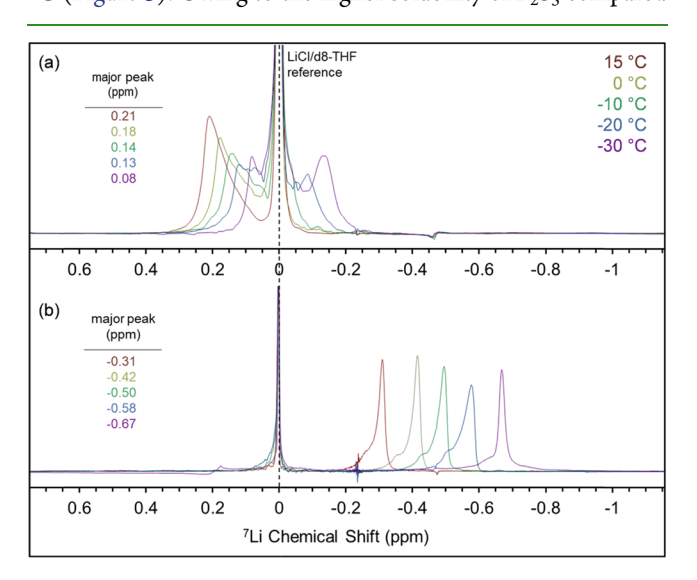


Figure 5. Variable-temperature ⁷Li NMR of (a) 0.1 M Li₂S₄ and (b) 0.033 M P_2S_5 + 0.1 M Li_2S_4 from 15 to -30 °C. The peak for the Li₂S₄ solution at 15 °C broadens and new peaks are observed at reduced temperatures. In contrast, the peak for $P_2S_5 + Li_2S_4$ retains a similar profile at all temperatures, suggesting a unique electrostatic coordination environment for Li+. Chemical shifts are calibrated to the LiCl/d₈-tetrahydrofuran (THF) reference peak (dotted line).

to Li₃PS₄, we generated the thiophosphate-polysulfide group from the reaction of P₂S₅ with Li₂S₄. Confirming a reaction occurs between P2S5 and polysulfides, 31P NMR data (Figure S8) show signals above 50 ppm for various thiophosphate ions. 34,35

As temperature is reduced, the broad peak in the ⁷Li NMR spectra of Li₂S₄ in the absence of thiophosphate splits into multiple features and shifts upfield (Figure 5a). The emerging peaks, which become prominent by -10 °C, indicate multiple

electrostatic coordination environments for Li⁺. This observation has previously been attributed to polysulfide clustering, which is believed to be responsible for diffusion limitations and typically coincides with poor performance such as the lack of a lower discharge plateau at reduced temperatures. 9,29,36 Conversely, the NMR spectra for the Li₂S₄ + P₂S₅ solution exhibit a similar peak profile across the temperature range as the peaks shift upfield (Figure 5b). The lack of change in the peak profile suggests that the electrostatic coordination environment for Li+ in the presence of thiophosphates is similar at these temperatures and distinct from that of the clustered polysulfide environment seen without thiophosphates. The upfield shifts arise from increased shielding as the coordination environment for Li⁺ tightens in colder temperatures. Similar electrostatic effects imparted by solvent, cation, anion, and solute concentrations have previously been shown to disrupt polysulfide clustering and lead to improvements in electrochemical cycling performance reminiscent of those we have observed in this study. 29,36,37

The field of low-temperature Li-S battery research is nascent at this time, but it represents an area with immense potential to impact future electric vehicles ranging from cars to aircraft and spacecraft. In this work, we demonstrated that the covalent tethering of polysulfides to lithium thiophosphates (LPS) in MOF cathode additives is a promising method to improve the Li-S battery performance at reduced temperatures. M8-LPS, possessing the greatest concentration of LPS in this study, permitted the best low-temperature performance with the delivery of more than 800 mAh g^{-1} even at -10 °C. Importantly, the cells containing LPS were capable of ameliorating polarization and altering redox mechanisms with new features appearing in both low-temperature galvanostatic and voltammetric experiments. ⁷Li NMR spectra further elucidate the influence of thiophosphates on the Li-S chemistry. Ultimately, we believe that chemical tethering techniques represent a promising approach for further exploration of low-temperature Li-S performance. Further studies featuring other sulfur-anchoring cathode formulations, as well as fundamental studies of polysulfide behavior at low temperatures, are promising directions for this emerging research area.

ASSOCIATED CONTENT

Supporting Information

The Supporting Information is available free of charge at https://pubs.acs.org/doi/10.1021/acsami.1c12129.

Information regarding the preparation of materials and instrumental methods are provided along with supplementary electrochemical data, and photographs of the low-temperature cycling chamber (PDF)

AUTHOR INFORMATION

Corresponding Author

V. Sara Thoi — Department of Chemistry and Department of Materials Science and Engineering, Johns Hopkins University, Baltimore, Maryland 21218, United States; oorcid.org/0000-0003-0896-4077; Email: sarathoi@jhu.edu

Authors

- David A. Burns Department of Chemistry, Johns Hopkins University, Baltimore, Maryland 21218, United States; orcid.org/0000-0002-5067-5511
- Avery E. Baumann Department of Chemistry, Johns Hopkins University, Baltimore, Maryland 21218, United States; Ocid.org/0000-0001-8513-8049
- Kevin J. Bennett Department of Chemistry, Johns Hopkins University, Baltimore, Maryland 21218, United States José C. Díaz – Department of Chemistry, Johns Hopkins University, Baltimore, Maryland 21218, United States

Complete contact information is available at: https://pubs.acs.org/10.1021/acsami.1c12129

Author Contributions

§D.A.B. and A.E.B. contributed equally to this work.

Notes

The authors declare no competing financial interest.

ACKNOWLEDGMENTS

We acknowledge the financial support of the Division of Materials Research at the National Science Foundation (Award #1945114) and a Space@Hopkins seed grant from Johns Hopkins University. We thank Dr. Jonathan Catazaro (Johns Hopkins University) for assistance in variable-temperature NMR experiments. D.A.B. and A.E.B. both are grateful to receive Harry and Cleio Greer Fellowships from the Department of Chemistry. A.E.B. also acknowledges support from the ARCS Foundation for the Metropolitan Washington Chapter Scholar Award.

REFERENCES

- (1) Dong, X.; Guo, Z.; Guo, Z.; Wang, Y.; Xia, Y. Organic Batteries Operated at -70 °C. *Joule* **2018**, 2, 902–913.
- (2) Zhang, S.; Xu, K.; Jow, T. A New Approach toward Improved Low Temperature Performance of Li-Ion Battery. *Electrochem. Commun.* **2002**, *4*, 928–932.
- (3) Yuksel, T.; Michalek, J. J. Effects of Regional Temperature on Electric Vehicle Efficiency, Range, and Emissions in the United States. *Environ. Sci. Technol.* **2015**, *49*, 3974–3980.
- (4) Hu, X.; Zheng, Y.; Howey, D. A.; Perez, H.; Foley, A.; Pecht, M. Battery Warm-up Methodologies at Subzero Temperatures for Automotive Applications: Recent Advances and Perspectives. *Prog. Energy Combust. Sci.* **2020**, 77, No. 100806.
- (5) Rosenman, A.; Markevich, E.; Salitra, G.; Aurbach, D.; Garsuch, A.; Chesneau, F. F. Review on Li-Sulfur Battery Systems: An Integral Perspective. *Adv. Energy Mater.* **2015**, *5*, No. 1500212.
- (6) Manthiram, A.; Fu, Y.; Chung, S.-H.; Zu, C.; Su, Y.-S. Rechargeable Lithium—Sulfur Batteries. *Chem. Rev.* **2014**, *114*, 11751—11787.
- (7) Mikhaylik, Y. V.; Akridge, J. R. Low Temperature Performance of Li/S Batteries. J. Electrochem. Soc. 2003, 150, A306–A311.

- (8) Sun, K.; Li, N.; Su, D.; Gan, H. Electrolyte Concentration Effect on Sulfur Utilization of Li-S Batteries. *J. Electrochem. Soc.* **2019**, *166*, A50–A58.
- (9) Gupta, A.; Bhargav, A.; Jones, J.-P.; Bugga, R. V.; Manthiram, A. Influence of Lithium Polysulfide Clustering on the Kinetics of Electrochemical Conversion in Lithium–Sulfur Batteries. *Chem. Mater.* **2020**, 32, 2070–2077.
- (10) Ryu, H.-S.; Ahn, H.-J.; Kim, K.-W.; Ahn, J.-H.; Cho, K.-K.; Nam, T.-H.; Kim, J.-U.; Cho, G.-B. Discharge Behavior of Lithium/ Sulfur Cell with TEGDME Based Electrolyte at Low Temperature. *J. Power Sources* **2006**, *163*, 201–206.
- (11) Deng, D. R.; Xue, F.; Bai, C.-D.; Lei, J.; Yuan, R.; Zheng, M.; Sen Dong, Q. F. Enhanced Adsorptions to Polysulfides on Graphene-Supported BN Nanosheets with Excellent Li-S Battery Performance in a Wide Temperature Range. ACS Nano 2018, 12, 11120–11129.
- (12) Zhu, S.; Wang, Y.; Jiang, J.; Yan, X.; Sun, D.; Jin, Y.; Nan, C.; Munakata, H.; Kanamura, K. Good Low-Temperature Properties of Nitrogen-Enriched Porous Carbon as Sulfur Hosts for High-Performance Li–S Batteries. ACS Appl. Mater. Interfaces 2016, 8, 17253–17259.
- (13) Zhang, Z.; Wang, Y.; Liu, J.; Sun, D.; Ma, X.; Jin, Y.; Cui, Y. A Multifunctional Graphene Oxide-Zn(II)-Triazole Complex for Improved Performance of Lithium-Sulfur Battery at Low Temperature. *Electrochim. Acta* **2018**, *271*, 58–66.
- (14) Wang, X.; Zhao, X.; Ma, C.; Yang, Z.; Chen, G.; Wang, L.; Yue, H.; Zhang, D.; Sun, Z. Electrospun Carbon Nanofibers with MnS Sulfiphilic Sites as Efficient Polysulfide Barriers for High-Performance Wide-Temperature-Range Li—S Batteries. *J. Mater. Chem. A* **2020**, *8*, 1212—1220.
- (15) Huang, J.-Q.; Liu, X.-F.; Zhang, Q.; Chen, C.-M.; Zhao, M.-Q.; Zhang, S.-M.; Zhu, W.; Qian, W.-Z.; Wei, F. Entrapment of Sulfur in Hierarchical Porous Graphene for Lithium–Sulfur Batteries with High Rate Performance from -40 to 60°C. *Nano Energy* **2013**, *2*, 314–321.
- (16) Fan, C.-Y.; Zheng, Y.-P.; Zhang, X.-H.; Shi, Y.-H.; Liu, S.-Y.; Wang, H.-C.; Wu, X.-L.; Sun, H.-Z.; Zhang, J.-P. High-Performance and Low-Temperature Lithium-Sulfur Batteries: Synergism of Thermodynamic and Kinetic Regulation. *Adv. Energy Mater.* **2018**, *8*, No. 1703638.
- (17) Wang, Y.; Xu, Y.; Ma, S.; Duan, R.; Zhao, Y.; Zhang, Y.; Liu, Z.; Li, C. Low Temperature Performance Enhancement of High-Safety Lithium—Sulfur Battery Enabled by Synergetic Adsorption and Catalysis. *Electrochim. Acta* **2020**, 353, No. 136470.
- (18) Zhou, Z.; Li, G.; Zhang, J.; Zhao, Y. Wide Working Temperature Range Rechargeable Lithium—Sulfur Batteries: A Critical Review. Adv. Funct. Mater. 2021, No. 2107136.
- (19) Yu, X.; Manthiram, A. Electrode-Electrolyte Interfaces in Lithium-Based Batteries. *Energy Environ. Sci.* **2018**, *11*, 527-543.
- (20) Yu, S.-H.; Huang, X.; Schwarz, K.; Huang, R.; Arias, T. A.; Brock, J. D.; Abruña, H. D. Direct Visualization of Sulfur Cathodes: New Insights into Li–S Batteries via Operando X-Ray Based Methods. *Energy Environ. Sci.* **2018**, *11*, 202–210.
- (21) Baumann, A. E.; Han, X.; Butala, M. M.; Thoi, V. S. Lithium Thiophosphate Functionalized Zirconium MOFs for Li-S Batteries with Enhanced Rate Capabilities. *J. Am. Chem. Soc.* **2019**, *141*, 17891–17899.
- (22) Xu, F.; Yang, S.; Chen, X.; Liu, Q.; Li, H.; Wang, H.; Wei, B.; Jiang, D. Energy-Storage Covalent Organic Frameworks: Improving Performance: Via Engineering Polysulfide Chains on Walls. *Chem. Sci.* **2019**, *10*, 6001–6006.
- (23) Baumann, A. E.; Downing, J. R.; Burns, D. A.; Hersam, M. C.; Thoi, V. S. Graphene—Metal—Organic Framework Composite Sulfur Electrodes for Li—S Batteries with High Volumetric Capacity. ACS Appl. Mater. Interfaces 2020, 12, 37173—37181.
- (24) Burns, D. A.; Benavidez, A.; Buckner, J. L.; Thoi, V. S. Maleimide-Functionalized Metal—Organic Framework for Polysulfide Tethering in Lithium—Sulfur Batteries. *Mater. Adv.* **2021**, *2*, 2966—2970.

- (25) Mikhaylik, Y. V.; Akridge, J. R. Polysulfide Shuttle Study in the Li/S Battery System. *J. Electrochem. Soc.* **2004**, *151*, A1969—A1976.
- (26) Zhao, M.; Li, B.-Q.; Zhang, X.-Q.; Huang, J.-Q.; Zhang, Q. A Perspective toward Practical Lithium—Sulfur Batteries. ACS Cent. Sci. 2020, 6, 1095–1104.
- (27) Gupta, A.; Manthiram, A. Designing Advanced Lithium-Based Batteries for Low-Temperature Conditions. *Adv. Energy Mater.* **2020**, *10*, No. 2001972.
- (28) Jeong, S. S.; Lim, Y. T.; Choi, Y. J.; Cho, G. B.; Kim, K. W.; Ahn, H. J.; Cho, K. K. Electrochemical Properties of Lithium Sulfur Cells Using PEO Polymer Electrolytes Prepared under Three Different Mixing Conditions. *J. Power Sources* **2007**, *174*, 745–750.
- (29) Gupta, A.; Bhargav, A.; Manthiram, A. Tailoring Lithium Polysulfide Coordination and Clustering Behavior through Cationic Electrostatic Competition. *Chem. Mater.* **2021**, *33*, 3457–3466.
- (30) Lin, Z.; Liu, Z.; Fu, W.; Dudney, N. J.; Liang, C. Phosphorous Pentasulfide as a Novel Additive for High-Performance Lithium-Sulfur Batteries. *Adv. Funct. Mater.* **2013**, 23, 1064–1069.
- (31) Busche, M. R.; Adelhelm, P.; Sommer, H.; Schneider, H.; Leitner, K.; Janek, J. Systematical Electrochemical Study on the Parasitic Shuttle-Effect in Lithium-Sulfur-Cells at Different Temperatures and Different Rates. *J. Power Sources* **2014**, 259, 289–299.
- (32) Dibden, J. W.; Meddings, N.; Owen, J. R.; Garcia-Araez, N. Quantitative Galvanostatic Intermittent Titration Technique for the Analysis of a Model System with Applications in Lithium—Sulfur Batteries. ChemElectroChem 2018, 5, 445—454.
- (33) Zhang, N.; Yang, Y.; Feng, X.; Yu, S.-H.; Seok, J.; Muller, D. A.; Abruña, H. D. Sulfur Encapsulation by MOF-Derived CoS 2 Embedded in Carbon Hosts for High-Performance Li–S Batteries. *J. Mater. Chem. A* **2019**, *7*, 21128–21139.
- (34) Dietrich, C.; Weber, D. A.; Culver, S.; Senyshyn, A.; Sedlmaier, S. J.; Indris, S.; Janek, J.; Zeier, W. G. Synthesis, Structural Characterization, and Lithium Ion Conductivity of the Lithium Thiophosphate $\text{Li}_2\text{P}_2\text{S}_6$. Inorg. Chem. **2017**, 56, 6681–6687.
- (35) Dietrich, C.; Weber, D. A.; Sedlmaier, S. J.; Indris, S.; Culver, S. P.; Walter, D.; Janek, J.; Zeier, W. G. Lithium ion conductivity in Li₂S-P₂S₅ glasses building units and local structure evolution during the crystallization of superionic conductors Li₃PS₄, Li₇P₃S₁₁ and Li₄P2S₇. *J. Mater. Chem. A* **2017**, *5*, 18111–18119.
- (36) Gupta, A.; Manthiram, A. Unifying the clustering kinetics of lithium polysulfides with the nucleation behavior of Li_2S in lithium—sulfur batteries. *J. Mater. Chem. A* **2021**, *9*, 13242–13251.
- (37) Rajput, N. N.; Murugesan, V.; Shin, Y.; Han, K. S.; Lau, K. C.; Chen, J.; Liu, J.; Curtiss, L. A.; Mueller, K. T.; Persson, K. A. Elucidating the Solvation Structure and Dynamics of Lithium Polysulfides Resulting from Competitive Salt and Solvent Interactions. *Chem. Mater.* **2017**, *29*, 3375–3379.